

Investigation of Performance of Semi-Circular Blades in Savonius Rotor

S. K. Dhiman

(Department of Mechanical Engineering
Birla Institute of Technology, Mesra, Ranchi, India)

Abstract

The paper aims to investigate the performance of semi-circular blade geometry of a Savonius rotor to achieve the optimum output from it. Experiments were conducted to measure rotor speed and torque while the power and torque coefficients were calculated. Three upwind air velocities were taken viz. 8.68 m/s, 10.26 m/s and 12.33 m/s. The overlap ratios were varied as: 0.1, 0.2, 0.3, 0.4 and 0.5 for four different aspect ratios viz. 0.7, 0.75, 0.775 and 0.8. Results showed that the optimum power and torque coefficients are dependent on overlap ratio and aspect ratio. Overlap ratio between 0.2-0.25 and aspect ratio between 0.75-0.775 showed the optimum condition of output.

Keywords - savonius rotor, Semi-circular blades, overlap ratio, aspect ratio

I. INTRODUCTION

Since few decades, interest of utilization of wind energy has been growing and many researchers have attempted to introduce cost-effective, reliable wind energy conversion systems all over the world. However, many difficulties encounter to introduce wind energy conversion systems to the community because of less wind energy source, profitability, noise emission, etc. Therefore, researchers are putting efforts to utilize maximum of available energy in the wind using horizontal and vertical axes of the rotor and to design blade profiles for the same. The application of wind energy conversion systems is now no more limited to developing area, where lots of people do not yet have access to conventional electricity service, but also to an urban area where one can make better living space for future generation. In the present paper, investigation of Savonius wind turbine blade profiles at available wind velocity of 8, 12 and 16.5 m/s is shown.

Savonius wind turbines are a type of vertical-axis wind turbine (VAWT), used for converting the power of wind to torque on a rotating shaft. Savonius turbines are one of the simplest turbines. Savonius rotor is simple in structure, has good starting characteristics, relatively low operating speed, relatively low construction cost and ability to accept wind from any direction. However, it has low efficiency. Aerodynamically, they are drag-type

devices, consisting of two or three scoops. Because of curvature, scoops experiences less drag when moving against wind than when moving with wind. Differential drag causes Savonius rotor to spin. Because they are drag-type devices, Savonius rotor extract much less of wind's power than other similar-sized lift-type turbines.

S.J.Savonius initially developed vertical axis Savonius rotor in late 1920s [1]. The concept of Savonius rotor is based on the principle developed by Fletter, which is such that, cutting a vertical cylinder longitudinally into two halves along the central plane and shifting semi cylindrical surfaces in opposite directions along the cutting plane, that cross section resembled the letter 'S' (figure 1). Savonius tested more than 30 different models of Savonius rotors in wind tunnel to determine the best geometry and reported very encouraging results. Also, he conducted tests in natural wind and reported that Savonius rotor would run at a higher speed in natural wind than in the wind tunnel for the same wind velocity. Best of rotor models he tested had the efficiency of 31% while maximum reported efficiency of the prototype was 37%.

Investigation of J.L. Menet[2] deals with the conception of a small Savonius rotor (i.e. of low power) for local production of electricity. The data were calculated on the basis of nominal wind velocity of 10m/s. Whole design of prototype has confirmed the high efficiency and low technicality of Savonius rotors for local production of electricity. Saha et al.[3], conducted a wind tunnel test to assess an aerodynamic performance of single, two and three stage Savonius rotors to optimize the parameters like number of stages, number of blades and blade geometry. They took circular profile of blades. Investigation of Altan et al.[4], introduces a new curtaining arrangement to improve the performance of Savonius rotors. Curtain arrangement was placed in front of the rotor preventing the negative torque opposite the rotor rotation. The geometrical parameters of curtain arrangement were optimized to generate an optimum performance. Rotor with different curtain arrangements was tested out of a wind tunnel, and its performance was compared with that of the conventional rotor. Maximum power

Figure 3: Rotor Blades

The experimental set-up is placed at a distance of 750 mm downstream of the blower exit such that longitudinal axis of the blower pipe passes through the center of gravity of the rotor. The measured velocity distribution at the rotor position is uniform within $\pm 1\%$ in the central area of 254 mm \times 254 mm. The turbulence intensity at the rotor position is estimated to be 1%.

Experimental set-up for conducting rotational experiments consists of a structure housing the modified Savonius rotor fabricated using studs and mild steel plates (figure3). The mild steel plates are held in place by means of washers and nuts. Two bearings (6304-2RS1 S.K.F.) bolted to the mild steel plates support the modified Savonius rotor. The usage of studs, nuts and bolts facilitated easy replacement of rotors of different diameters and positioning of rotor center at the center of the wind tunnel.

Friction is an important parameter that affects the measurement of torque of the rotating Savonius rotor. Friction in the bearings and the 12 mm leather belt wound on the rotor shaft must be minimized. The seals are removed from the bearings and bearings are washed in petrol to remove the grease before mounting resulting in the reduction of friction. Wind velocity is measured with help of Anemometer (make: Ogawa Siki Co.Ltd. Tokyo Central) shown in figure4. Wind velocity is adjusted corresponding to a required velocity by the various orifice present in the Measurement laboratory of Department of Mechanical Engineering, Birla Institute of Technology, Mesra Ranchi. Rotor is allowed to rotate from no load speed. Rotational speed of the rotor is recorded by a non-contact type tachometer. Each bearing is sprayed with machine oil (a commercially available spray) lubricant before each reading. The rotor is loaded gradually to record spring balance reading, weights and rotational speed of the rotor.



Figure 4: Anemometer

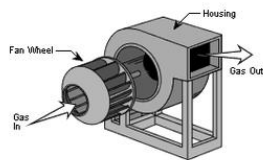


Figure 5: Centrifugal fan

III. ENERGY IN THE WIND

For an airstream flowing through an area A, the mass flow rate is ρAV , and therefore the dynamic power available in wind

$$P = \frac{1}{2} (\rho AV)V^2 = \frac{1}{2} \rho AV^3$$

where, ρ is the air density (kg/m³), V is the wind speed (m/s) at the blower exit and P is the dynamic power (Watts). The power is also known as the energy flux or power density of the air [2,7]. The

ratio of rotor power (Protor) to the dynamic power available in the wind (P) is known as the power coefficient (Cp), and this indicates the efficiency of conversion. Thus,

$$C_p = \frac{P_{rotor}}{P}$$

The performance of a wind rotor can be expressed in the form of power coefficient Cp versus tip-speed ratio λ and the torque coefficient Ct versus tip-speed ratio λ at various overlap ratio conditions. For the analysis the following relations has been used:

For a Savonius rotor of height H and radius R

$$C_p = \frac{P_{rotor}}{\frac{1}{2}\rho AV^3}$$

$$P_{rotor} = \left(\frac{1}{2}\rho AV^2\right) u = \left(\frac{1}{2}\rho AV^2\right) \frac{\pi DN}{60}$$

where, u is blade speed in m/s

$$T = \frac{60 P}{2\pi N}$$

$$C_t = \frac{T}{\left(\frac{1}{2}\rho AV^2\right) d}$$

$$\lambda = \frac{u}{V} = \frac{\omega R}{V} = \frac{\pi DN}{60 V}$$

$$C_p = \frac{P_{rotor}}{\frac{1}{2}\rho (H \times R)V^3}$$

here, A (= H x R) is the projected area.

$$C_t = \frac{T}{\left(\frac{1}{2}\rho H R V^2\right) d}$$

A centrifugal fan (also blower, or squirrel-cage fan, as it looks like a hamster wheel) is a mechanical device for moving air or other gases. It has a fan wheel composed of a number of fan blades, or ribs, mounted around a hub. As shown in figure 5, the hub turns on a driveshaft that passes through the fan housing. The gas enters from the side of the fan wheel, turns 90 degrees and accelerates due to centrifugal force as it flows over the fan blades and exits the fan housing. The fluid kinetic energy (velocity) is then converted to (static) pressure due to the change in area the fluid experiences in the volute section.

IV. RESULTS AND DISCUSSION

Figures 6-9 shows the variation of rotational speed (rpm) at three velocities 8.68 m/s, 10.26 m/s and 12.33 m/s for overlap ratios 0.1, 0.2, 0.3, 0.4 and 0.5 and aspect ratios 0.7, 0.75, 0.775 and 0.8. It is obvious that any rotating element when subject to increasingly upstream velocities gives the increasingly rotational speed. From the figures 13-16 it is apparent that the rotational speed increases with the velocity and is dependent greatly on overlap ratio. All the curves show that there is a very narrow range of overlap ratio 0.2 – 0.25, at which the rotational speed is maximum. This observation holds good for low velocities and diminishes with the velocity increase.

Figure 10-12 shows the variations of rotational speed at various overlap ratios with respect to aspect ratios at different upstream velocities. It is

again apparent in these figures that rotational speeds are higher for overlap ratio ranging 0.2-0.25. Further it has also been observed that at upstream velocity of 8.68 m/s rotational speeds increases with aspect ratio, arrive a peak value and then decreases. It has also been observed that the peak value of rotational speed comes out at aspect ratio = 0.77. The above observation of peak values is due to the high drag difference between concave and convex part of the blade surface. Figures 18 and 19 shows that, with increase in upstream velocity effect of drag difference diminishes.

Figures 13 – 15 shows the variation of rotational speed at various aspect ratios with respect to overlap ratios at different upstream velocities. As mentioned earlier that the overlap ratio has the range 0.2 - 0.25 and aspect ratio has the range 0.75 – 0.78 at which the speed of the rotor is maximum. Figure 20 gives the clear evidence of this and shows that at $\alpha = 0.775$ and overlap ratio of 0.24 the rotational speed would be always be maximum and is well validated with Manet [1].

Figures 16 – 18 shows the variations of Power Coefficient for all aspect ratios and overlap ratios taken. From figure 23 and 25 it is very clearly evident that power coefficient increases with aspect ratio and attains a maximum at 0.775 and then decreases while it has a peak value for overlap ratio 0.2. It also shows that as the overlap ratio increases further than 0.2 power coefficient decreases.

From power coefficient curve a success of 20% with standard deviation of ± 7.2 has been achieved compared with the literatures.

Figures 26 -28 shows the variations of torque coefficient for all aspect ratios with respect to overlap ratios at different upstream velocities. From the figures it has been observed that the effect variation of torque coefficient lies within 0.4 – 0.6 and an average value of torque coefficient comes out to be 0.52 with $\pm 2\%$ error. A similar trend in torque coefficient is observed as that of power coefficient with respect to overlap ratio and aspect ratio. Again from torque coefficient curve a success of 20% with standard deviation of ± 7.2 has been achieved compared with the literatures.

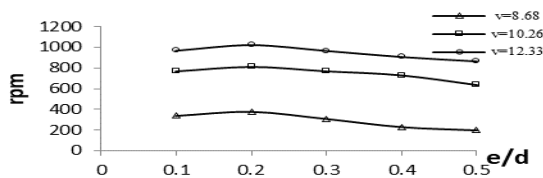


Figure 6: Variation of speed at three velocities vs overlap ratio for $\alpha = 0.7$

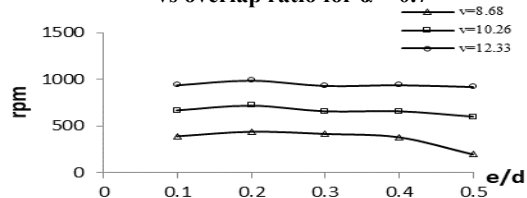


Figure 7: Variation of speed at three velocities vs overlap ratio for $\alpha = 0.75$

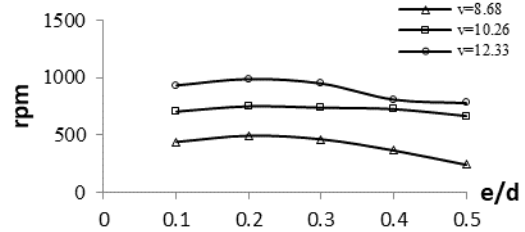


Figure 8: Variation of speed at three velocities vs overlap ratio for $\alpha = 0.775$

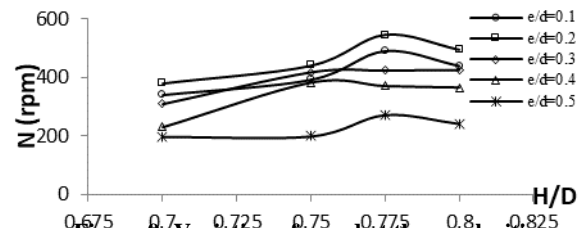


Figure 9: Variation of speed at three velocities vs overlap ratio for $H/D = 0.8$

Figure 10: Variation of Speed vs aspect ratio for various overlap ratios ($v = 8.68$ m/s)

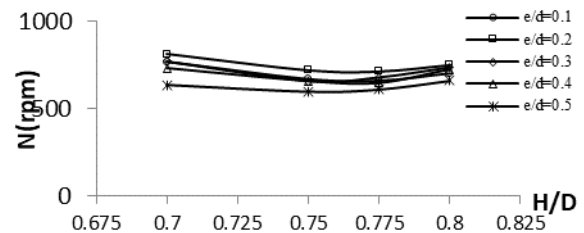
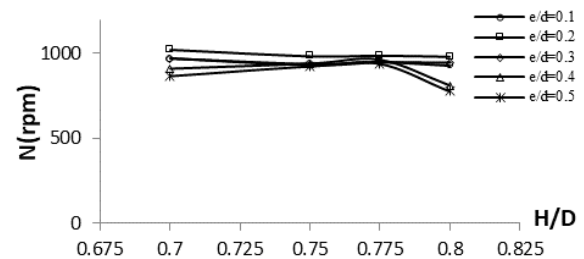


Figure 11: Variation of Speed vs aspect ratio for various overlap ratios ($v = 10.26$ m/s)



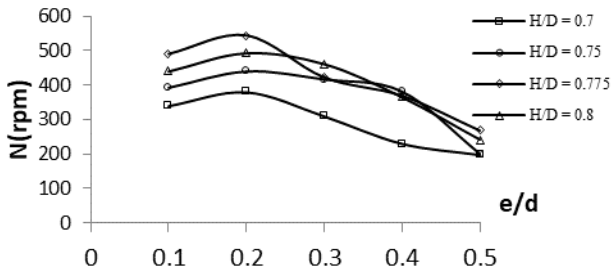


Figure 13: Variation of rotational speed at various aspect ratios vs overlap ratio (at $v =$)

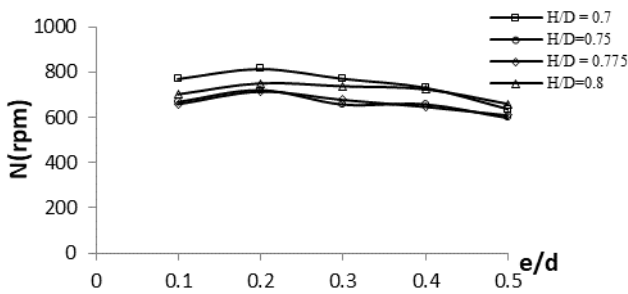


Figure 14: Variation of rotational speed at various aspect ratios vs overlap ratio (at $v =$)

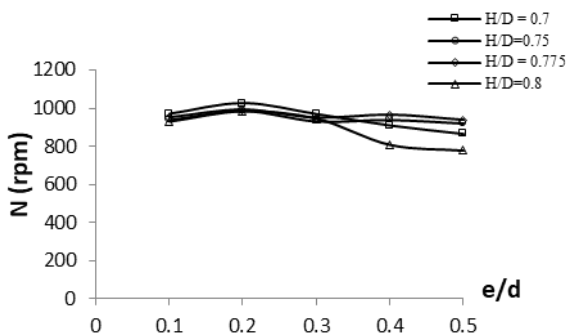


Figure 15: Variation of rotational speed at various aspect ratios vs overlap ratio (at $v =$)

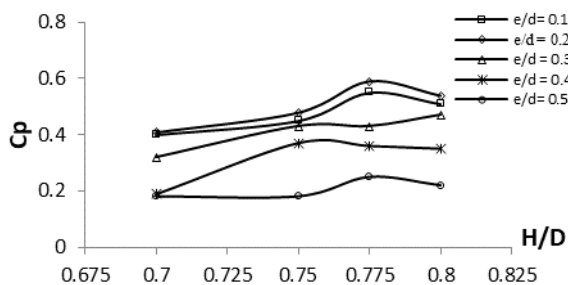


Figure 16: Variation of power coefficient vs aspect ratio for various overlap ratios (at $v =$)

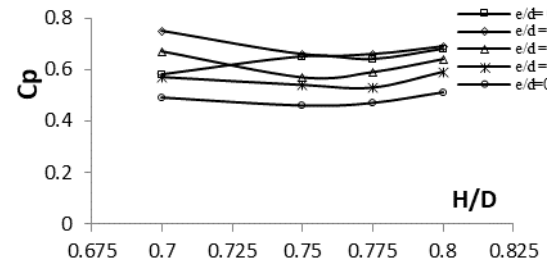


Figure 17: Variation of power coefficient vs aspect ratio for various overlap ratios (at $v =$)

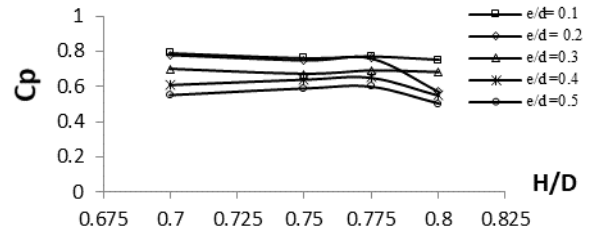


Figure 18: Variation of power coefficient vs aspect ratio for various overlap ratios (at $v =$)

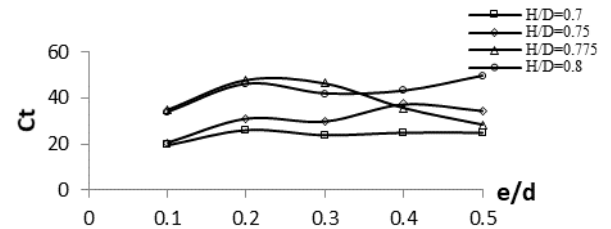


Figure 19: Variation of torque coefficient vs overlap ratio for various aspect ratios (at $v = 8.68$)

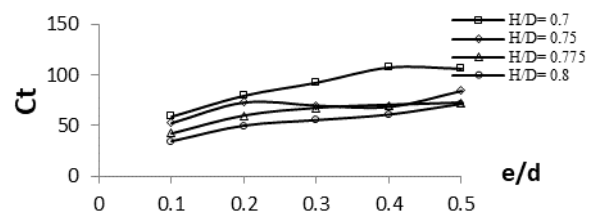


Figure 20: Variation of torque coefficient vs. overlap ratio for various aspect ratios (at $v =$)

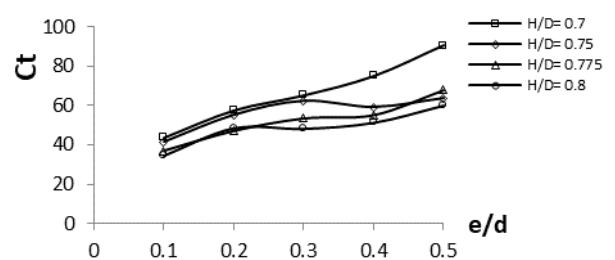


Figure 21: Variation of torque coefficient vs. overlap ratio for various aspect ratios (at $v =$

V. CONCLUSION

From the present experimental work it has been concluded that an overlap ratio within the range 0.2-0.25 and aspect ratio within the range 0.75-0.775 shows the optimum output of the blade geometry of the type under investigation.

Nomenclature

P = dynamic power (watts)
Pr = rotor power (watts)
Tr = rotor torque (watts)
Cp = power coefficient
Ct = torque coefficient
 ρ = density of air (kg/m³)
A = projected area of the blade for wind (m²)
R = radius of rotor (m)
H = blade height (m)
u = blade velocity (m/s)
N = blade speed (rpm)
e/d = overlap ratio
V = wind velocity (m/s)
 α = aspect ratio (H/D)

REFERENCES

- [1] Savonius SJ, "The S-rotor and its application". Mech Eng 53, 1931.
- [2] J.-L. Menet, "A double-step Savonius rotor for local production of electricity: a design study", Renewable Energy vol. 29 pp.1843–1862, 2004.
- [3] U.K. Saha, S. Thotla, and D. Maity, "Optimum design configuration of Savonius rotor through wind tunnel experiments", Journal of Wind Engineering and Industrial Aerodynamics, vol.96, pp.1359– 1375, 2008.
- [4] Burcin Deda Altan, Mehmet Atilgan, and Aydog an Ozdamar, "An experimental study on improvement of a Savonius rotor performance with curtaining", Experimental Thermal and Fluid Science vol. 32, pp.1673–1678, 21008.
- [5] R. Gupta, A. Biswas, and K.K. Sharma, "Comparative study of a three-bucket Savonius rotor with a combined three-bucket Savonius–three-bladed Darrieus rotor", Renewable Energy, vol. 33, pp.1974–1981, 2008.
- [6] M.A. Kamoji, S.B. Kedare, and S.V. Prabhu, "Performance tests on helical Savonius rotors", Renewable Energy, vol.34, pp.521–529, 2009.
- [7] R.C. Bansal, T.S. Bhatti, and D.P. Kothari, "On some design aspects of wind energy conversion systems", Energy Convers. Manage, vol.43, pp.2175–2187, 2002.
- [8] I. Ushiyama and H. Nagai, "Optimum design configurations and performances of Savonius rotors", Wind Eng. Vol.12(1), pp.59–75, 1988.